

## **Electronic Supplementary Information**

### **Aqueous light-driven hydrogen production by a Ru-Ferredoxin-Co biohybrid**

Sarah R. Soltau,<sup>1</sup> Jens Niklas,<sup>1</sup> Peter D. Dahlberg,<sup>1,2</sup> Oleg G. Poluektov,<sup>1</sup> David M. Tiede,<sup>1</sup>  
Karen L. Mulfort,<sup>1</sup> and Lisa M. Utschig<sup>1,\*</sup>

<sup>1</sup>Chemical Sciences and Engineering Division, Argonne National Laboratory, Argonne, Illinois  
60439, United States

<sup>2</sup>Graduate Program in the Biophysical Sciences, The University of Chicago, Chicago, Illinois  
60637, United States

Email: [utschig@anl.gov](mailto:utschig@anl.gov)

#### Contents:

Experimental	S2
Tables	S8
Figures	S9
References	S23

## Experimental

*Synthesis and characterization.* Chemicals for the synthesis of Co and PS were purchased from Sigma-Aldrich and used as received. The cobaloxime catalyst,  $\text{Co}(\text{dmgBF}_2)_2 \cdot 2\text{H}_2\text{O}$  (Co), was synthesized and characterized according to published methods.<sup>1</sup> The ruthenium photosensitizer (PS),  $[\text{Ru}(4\text{-CH}_2\text{Br-4'-CH}_3\text{-2,2'-bpy})(\text{bpy})_2] \cdot 2\text{PF}_6$ , was also synthesized and characterized according to published methods.<sup>2</sup> Aqueous cyclic voltammetry of the Co catalyst was performed using a standard three-electrode cell on a BAS 100B potentiostat using a 3 mm diameter glassy carbon working electrode, a Pt wire auxiliary electrode, and Ag/AgCl reference electrode (3M KCl). The catalyst was dissolved in 10 mM MES buffer pH 6.3 with 100 mM potassium chloride added as an electrolyte. Peaks were referenced to ferrocene carboxylic acid as an internal standard.<sup>3</sup> All scans were performed at 100 mV/s. UV-vis and EPR samples of  $[\text{Ru}(\text{bpy})_3]^{3+}$  were prepared by oxidation of  $\text{Ru}(\text{bpy})_3\text{Cl}_2$  with  $\text{PbO}_2$  in 0.05M aqueous  $\text{H}_2\text{SO}_4$  according to literature procedures.<sup>4</sup> Glycerol (30% v/v) was added to the sample for EPR analysis to obtain a transparent glass at 10K.

*Preparation of Ru-Fd-Co hybrid.* The Ru-Fd-Co hybrids were prepared using *Spinacia oleracea* ferredoxin (Fd) from Sigma-Aldrich. Spinach Fd was dissolved in 20 mM HEPES buffer pH 7.9 and washed 4-5 times with Amicon 3000 MWCO filtration devices to remove all residual salt and concentrate the sample to 1-2 mM Fd. Fd-Co hybrids were prepared by the addition of 4 mol equiv. of Co (from a freshly prepared 3-5 mM stock solution of Co catalyst in DMSO) to 100-500  $\mu\text{M}$  Fd in 20 mM HEPES pH 7.9. The Fd-Co complex was tumbled (Labquake rotisserie) for 2 h at room temperature in the dark. Samples were concentrated with Amicon 3000 MWCO filtration devices and repeatedly diluted and washed at least 4 times with 20 mM HEPES pH 7.9 to remove unbound Co catalyst. The Ru-Fd-Co hybrid was prepared by the

addition of the 2 mol equiv. Ru PS to the Fd-Co complexes. Ru PS from a stock solution (3-5 mM in DMSO) was added directly to a 100-250  $\mu$ M Fd-Co hybrid in 20 mM Hepes pH 7.9. Ru-Fd-Co hybrids were tumbled for 2 h at room temperature in the dark. Samples were concentrated with Amicon 3000 MWCO filtration devices and repeatedly diluted (at least 5 times) with 20 mM Hepes pH 7.9 to remove the unbound Ru PS. Ru-Fd samples were prepared in the same manner as Fd-Co hybrid samples with addition of the Ru 2:1 with respect to the Fd concentration (100-250  $\mu$ M Fd). Inductively coupled plasma atomic emission spectroscopy (ICP-AES) with a Thermo Scientific iCAP6000 spectrometer was performed to determine Co, Fe, and Ru content in each sample. Fd protein concentration was extrapolated using UV-visible absorption and a molar extinction coefficient of 9600  $M^{-1}cm^{-1}$  at 422 nm.<sup>5</sup> Sephadex G25 gel filtration chromatography was also used to separate bound from unbound Ru PS and Co in Ru-Fd-Co sample preparation protocols. Metal analysis following chromatography demonstrated similar binding profiles of Co and Ru to Fd to those obtained with microfiltration techniques. 5,5'-Dithio-bis(2-nitrobenzoic acid) (DTNB) was used to quantify free cysteine residues in Fd. 25  $\mu$ M Fd was incubated with 250  $\mu$ M DTNB in 20 mM TAPS pH 8.5 for 30 minutes and Cys content was determined using the concentration 2-nitro-5-thiobenzoate anion ( $\epsilon_{412} = 14,150 M^{-1}cm^{-1}$ ). 1.0 Free Cys residues / Fd were detected by DTNB binding. The DTNB bound Fd was equilibrated with 10 mol equiv. of Ru PS and tumbled for 1.5 h in the dark at room temperature to allow time for binding. The sample was then extensively washed with 3000 MWCO filtration devices to remove all unbound Ru PS. Metal content analysis of these samples indicated <0.1 Ru/Fd.

*Preparation of Ru-ApoFd-Co hybrid.* ApoFd was prepared by treatment of spinach Fd with 3% trichloroacetic acid and dithiothreitol as was reported for apo-flavodoxin with minor

modifications.<sup>6</sup> Upon precipitation of the apoprotein by centrifugation, the white protein pellets were resuspended with a buffered solution of Ru PS (20 mM Hepes pH 7.9) at a concentration of 10-50  $\mu$ M (1 Fd: 10 Ru) and tumbled in the dark at 4°C overnight. Microfiltration with Amicon 3000 MWCO membrane filters was then used to remove unbound Ru PS and the sample was repeatedly diluted and washed > 5 times with 20 mM Hepes pH 7.9. The ApoFd protein concentration was determined by the Bradford method.<sup>7</sup> 4 mol equiv. of Co catalyst (3-5 mM in DMSO) was added to Ru-ApoFd complex and tumbled in the dark at room temperature for 2 h. Further microfiltration with 3000 MWCO membrane filters was used to remove unbound Co catalyst. ApoFd was prepared by resuspension in 20 mM Hepes pH 7.9 directly in control experiments, where metal binding was not desired. ICP-AES was used to determine the Co, Fe, and Ru content of each sample.

*H<sub>2</sub> generation samples and measurements.* H<sub>2</sub> photocatalysis experiments were performed using 3.8 mL samples in a 5.3 mL spectrophotometer cell as has been previously described with minor modification.<sup>6, 8</sup> Samples were illuminated with a 300 W Xenon lamp (Perkin-Elmer) and the light was filtered with a 375 nm filter, a 29 cm water filter, and a low-pass filter (KG-1, Schott). Optimal H<sub>2</sub> production occurred with samples containing 1-5  $\mu$ M Ru-Fd-Co hybrid or 1-10  $\mu$ M Ru-ApoFd-Co hybrid (hybrid concentration determined by Fd concentration) with 100 mM sodium ascorbate as a sacrificial electron donor in 10 mM MES buffer pH 6.3. Other pH and buffer conditions were also attempted (pH 4.0-pH 10.0, acetate, Hepes, and CAPS buffers). None gave greater rates of turnover than 10 mM MES pH 6.3, and extreme pH values resulted no H<sub>2</sub> production using 2  $\mu$ M hybrid and 100 mM ascorbate. The pH of the reaction was monitored during photocatalysis and observed to increase only slightly (< 1 pH unit). The addition of acid to return the reaction to pH 6.3 did not increase the rate or duration of catalysis, suggesting that

H<sub>2</sub> production by the hybrid complex is not proton limited. The ascorbate and buffer solutions were purged with N<sub>2</sub> gas prior to the addition of the Ru-Fd-Co or Ru-ApoFd-Co hybrids in a nitrogen box. H<sub>2</sub> evolution was determined by sampling aliquots of the 1.5 mL headspace by gas chromatography using a Varian CP-4900A GC with a 10m 5-Å molecular sieves column with a thermal conductivity detector and UHP N<sub>2</sub> carrier gas. H<sub>2</sub> production from the GC was calibrated using a standard curve prepared from aliquots of 3% H<sub>2</sub> in N<sub>2</sub> gas mixture.

*Transient optical spectroscopy samples and measurements.* Transient optical spectroscopy samples were prepared the same as other Ru-Fd-Co, Ru-ApoFd-Co, or Ru-ApoFd samples. These samples were prepared at 250-300 μM in 20 mM Hepes pH 7.9 to provide sufficient optical density ( $A_{450} \sim 0.3-0.4$ ) in a 2 mm sealed sample cell. Samples were bubbled with N<sub>2</sub> for at least 15 minutes before excitation. Aliquots of sodium ascorbate (200 mM) were injected into the samples immediately before excitation. Instrument response was calibrated against a sample of [Ru(bpy)<sub>3</sub>]<sub>2</sub>PF<sub>6</sub>, prepared to the equivalent optical density ( $A_{450} \sim 0.4$ ), with and without 200 mM sodium ascorbate. Samples were excited at 10 Hz with the output of an OPO pumped with a frequency doubled YAG (Continuum Surelight). The power per pulse at the sample was  $\sim 2$  mJ/cm<sup>2</sup>. A Thorlabs LED (M660L3) centered at 660 nm was used to probe the sample and the transient signal was detected using a monochromator (Jobin YVON TRIAX) and a PMT recorded with a digital oscilloscope (PicoScope 4227). Signals were averaged 1000 times for each sample and collected over approximately 10 minutes. A 72 ns sampling interval was used to collect the [Ru(bpy)<sub>3</sub>]<sup>2+</sup> and Ru-ApoFd kinetic traces shown in Figures 3A inset and S8-S9. For observation of slower kinetic states (i.e. Co(I)), the sample interval was increased from 72 ns to 2300 ns (Figure 3A-B)). This large integration time on the detector improves signal-to-noise, allows sampling to longer times, but convolves and distorts the fast dynamics.

Data in Figure S6 was collected at the Center for Nanoscale Materials at Argonne National Laboratory to collect full spectral transient optical measurements. The data was collected using an amplified Ti:sapphire laser system (Spectra Physics, Spitfire Prof) and automated data collection system (Ultrafast Systems, EOS for 0-100  $\mu$ s) using 1.0 kHz pulse and a supercontinuum light source (Ultrafast Systems) as the probe. The pump wavelength was 450 nm and pump power was 600  $\mu$ W. Sample intensity was  $\sim$ 0.3 OD at 450 nm and required  $\sim$ 24 h of signal averaging due to long sample lifetimes.

*Protein samples for EPR measurements.* Fd-Co, Ru-Fd, and Ru-Fd-Co hybrids were prepared aerobically as described above, in 20 mM Hepes buffer pH 7.9 to stabilize catalyst-protein covalent interactions with final Fd concentrations  $\sim$ 400  $\mu$ M. 100 mM sodium ascorbate was added to appropriate samples after removal of unbound metal ions by filtration. Samples of reduced Fd were prepared with 400  $\mu$ M protein in 100 mM CAPS buffer, pH 10.0 with 10 mM sodium dithionite. Samples ( $\sim$ 100-150  $\mu$ l) were placed in a N<sub>2</sub> box and equilibrated to the box atmosphere for at least 15 min then bubbled with N<sub>2</sub> for 30 s. EPR tubes were bubbled with N<sub>2</sub> for at least 1 min, samples were added to the tube, and additional N<sub>2</sub> was blown into the sample for 1-2 min. Samples were septa-capped and frozen in liquid N<sub>2</sub>.

*X-band EPR measurements.* CW X-band (9 GHz) EPR experiments were carried out with a Bruker ELEXSYS E580 EPR spectrometer (Bruker Biospin, Rheinstetten, Germany), equipped with a super high Q resonator (Bruker ER 4122SHQE) and a helium gas-flow cryostat (ICE Oxford, UK). The temperature was controlled by an ITC (Oxford Instruments, UK). Illumination was performed with a 300 W Lamp (PE300F; Atlas Specialty Lighting, Tampa, FL). A combination of a 15cm water filter and a KG2 filter (Schott) minimized IR irradiation of the sample, while a 400 nm long pass filter (Schott) was used to block UV light.

*EPR spectral analysis and simulations.* Data processing was done using Xepr (Bruker BioSpin, Rheinstetten) and Matlab™ 7.11.2 (MathWorks) environment. The magnetic parameters were obtained from theoretical simulation of the EPR spectra using the EasySpin software package (version 4.5.5).<sup>9</sup> The relative accuracy in determination of the electronic g-tensor is estimated to be  $\pm 0.002$ . EPR analysis of the N- and O- bound contributions of the Co catalyst were determined as in the literature.<sup>10</sup>

**Table S1: H<sub>2</sub> Control Experiments**

Sample	H <sub>2</sub>	H <sub>2</sub>
	No	Yes
Co catalyst	X	
Ru PS	X	
Ru PS, Co catalyst	X	
[Ru(bpy) <sub>3</sub> ] <sup>2+</sup> , Co catalyst	X	
Fd	X	
Fd-Co hybrid	X	
Ru-Fd hybrid	X	
Ru-Fd-Co hybrid		X
Ru-Fd-Co hybrid without sodium ascorbate	X	
[Ru(bpy) <sub>3</sub> ] <sup>2+</sup> -Fd-Co hybrid	X	
ApoFd	X	
Ru-ApoFd-Co hybrid	X	

*S. oleracea* Ferredoxin (Fd) was used for all control experiments. All control experiments were performed in 10 mM MES pH 6.3 and 100 mM sodium ascorbate unless noted in the chart.

Illumination was performed as described in the experimental section above (*H<sub>2</sub> generation samples and measurements*) and samples were irradiated for at least 4 h or until cessation of H<sub>2</sub> production. Ru PS = [Ru(4-CH<sub>2</sub>Br-4'-CH<sub>3</sub>-2,2'-bpy) (bpy)<sub>2</sub>] $\cdot$ 2PF<sub>6</sub>, Co = Co(dmgbF<sub>2</sub>)<sub>2</sub> $\cdot$ 2H<sub>2</sub>O



## Figures

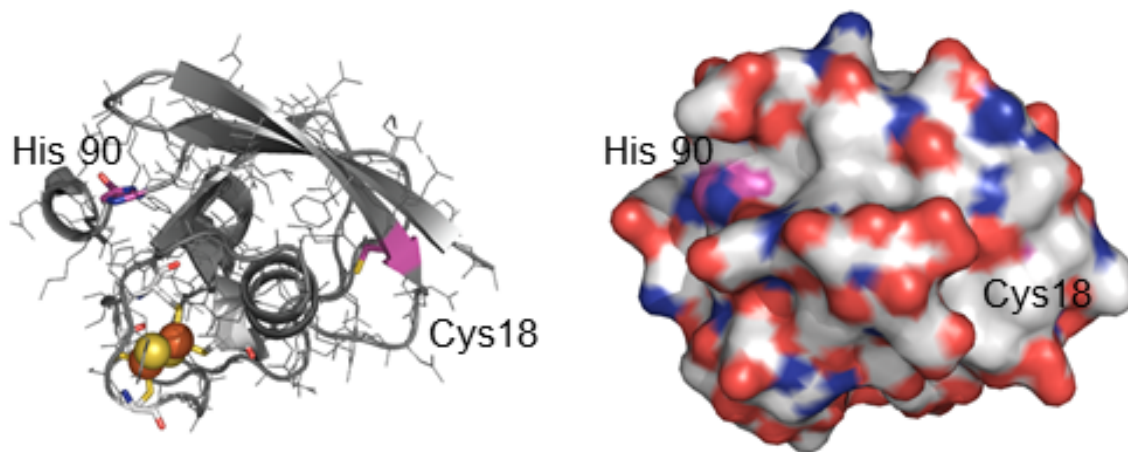


Figure S1: Cartoon and surface map of *S. oleracea* Fd indicating location of His 90 and Cys18 in magenta. His 90 is surface exposed, while Cys 18 is buried.

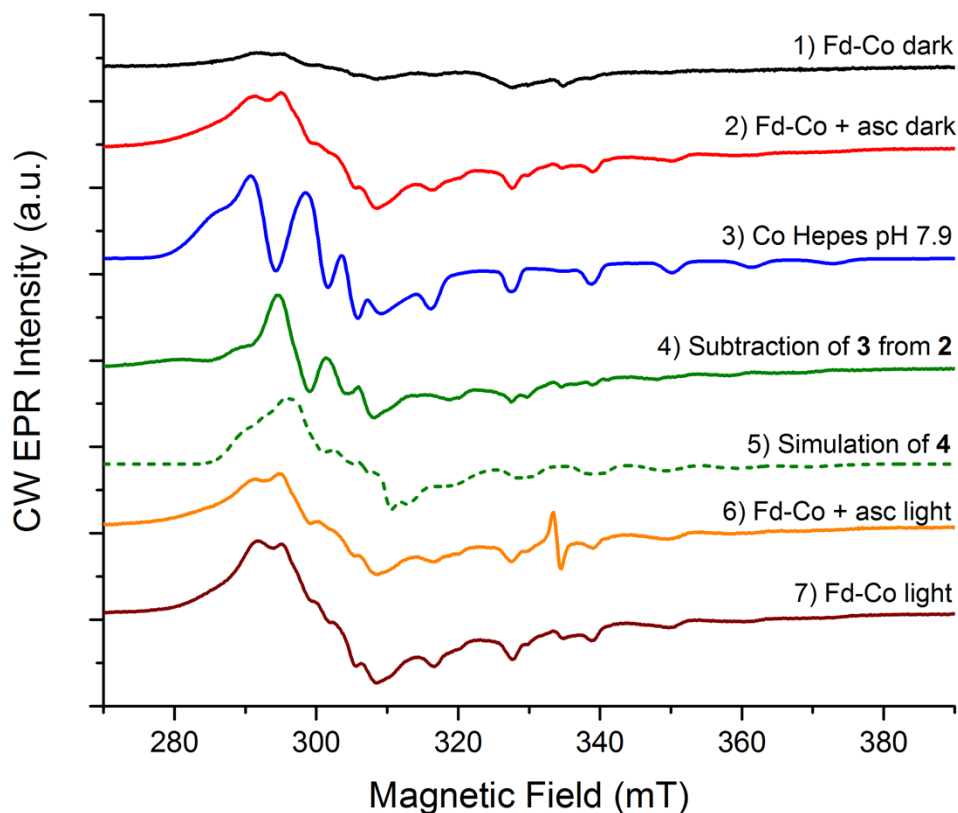


Figure S2: cw X-band EPR spectra of Fd-Co biohybrids. Fd-Co dark (black, 1), Fd-Co + ascorbate dark (red, 2), Co in Hepes buffer pH 7.9 (blue, 3), subtraction of 3 from 2 to give representative spectra of N-coordinated Co in Fd-Co hybrids (green, 4), simulation of 70% N-coordinated Co, (dashed green, 5), Fd-Co + ascorbate light (orange, 6), Fd-Co light (maroon, 7). “Light” samples were illuminated for 2 s at room temperature followed by immersion in liquid N<sub>2</sub> while illuminated and then placed in the pre-cooled EPR resonator for measurement. All EPR spectra were obtained at 10 K. Simulation parameters for 5 are provided in Figure S3.

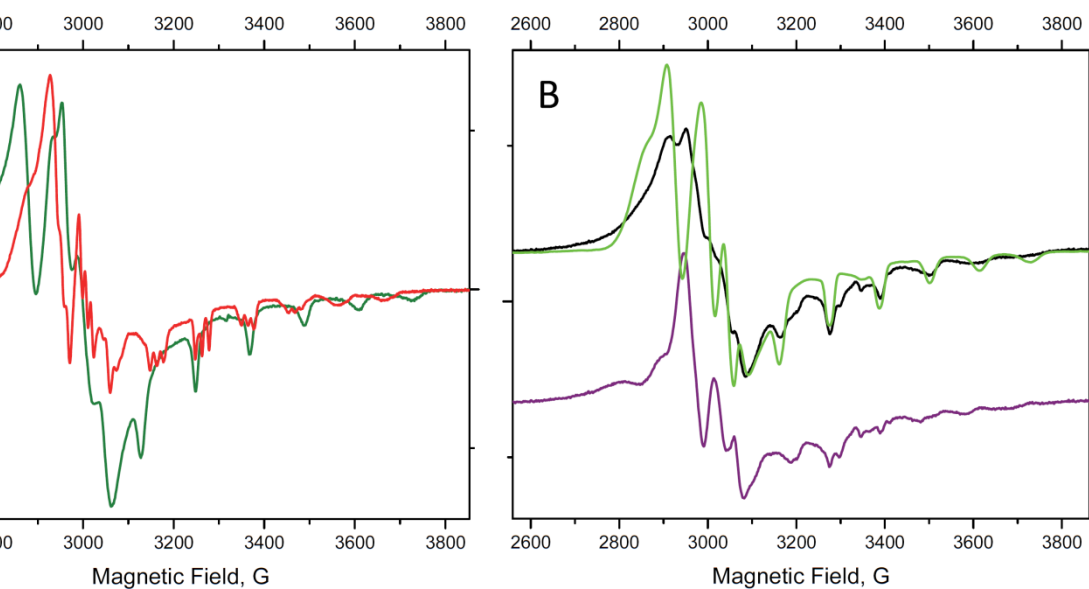


Figure S3. X-Band EPR of  $\text{CoBF}_2$  catalyst spectra with subtraction and simulation. A)  $\text{Co}(\text{dmgbf}_2)_2$  in methanol (green) and in methanol with pyridine/Co 1:1 (red). B) Fd-Co + ascorbate in HEPES pH 7.9 (black),  $\text{Co}(\text{dmgbf}_2)_2$  in HEPES pH 7.9 (green), and subtraction of green trace from black trace (purple). The EPR spectra were subtracted based on a published procedure.<sup>10</sup> Figure A shows two X-band EPR spectra of  $\text{BF}_2$ -capped cobaloximes with two axial oxygen ligands (green) and one axial nitrogen ligand (red). In addition to a difference in the

line shapes at low magnetic field, which is mainly due to differences in the  $g_x$  component of the  $g$ -tensors, there are also differences at high magnetic field region. Signals in the 3100-3800 G region are due to the hyperfine coupling (hfc) with  $^{59}\text{Co}$  ( $A_z$ -component) as well as hfc with one nitrogen of the axial ligand. Coupling with one nitrogen is revealed in splitting of each Co hyperfine line into triplet ( $I(^{14}\text{N})=1$ ). Note, the positions and line shape of the  $A_z$ -components are different for oxygen and nitrogen ligated spectra. This difference in the line shape (as a consequence of the different  $g$ - and  $A$ -parameters) was used to deconvolute the spectrum (B, black). This spectrum is overlapped with the spectrum of cobaloxime in the Hepes buffer (B, green). There is a clear difference in the low field and high field regions. Subtraction of green spectrum from the black spectrum was done in such a way as to remove all narrow peaks in the high field region (oxygen ligand) and at the same time remove strong lines at the low magnetic field. The best result is shown in B (purple). The theoretical simulation of the spectrum shown in Fig S2 (dashed green, 5). This spectrum was simulated with the following parameters:  $S = \frac{1}{2}$ ,  $g_x$ , 2.250;  $g_y$ , 2.158;  $g_z$ , 2.006;  $A_z$ , 280 MHz;  $A(^{14}\text{N}) = 39, 39, 43$  MHz. These parameters are in very good agreement with those reported for 1:1 Co : pyridine in methanol:  $g_x$ , 2.2380;  $g_y$ , 2.1530;  $g_z$ , 2.0058;  $A_z$ , 285 MHz. The average contribution of nitrogen ligated complexes to oxygen ligated is 70% : 30%. Note, intensities of the spectra in A and B are not normalized, but shown for a better comparison by eye.

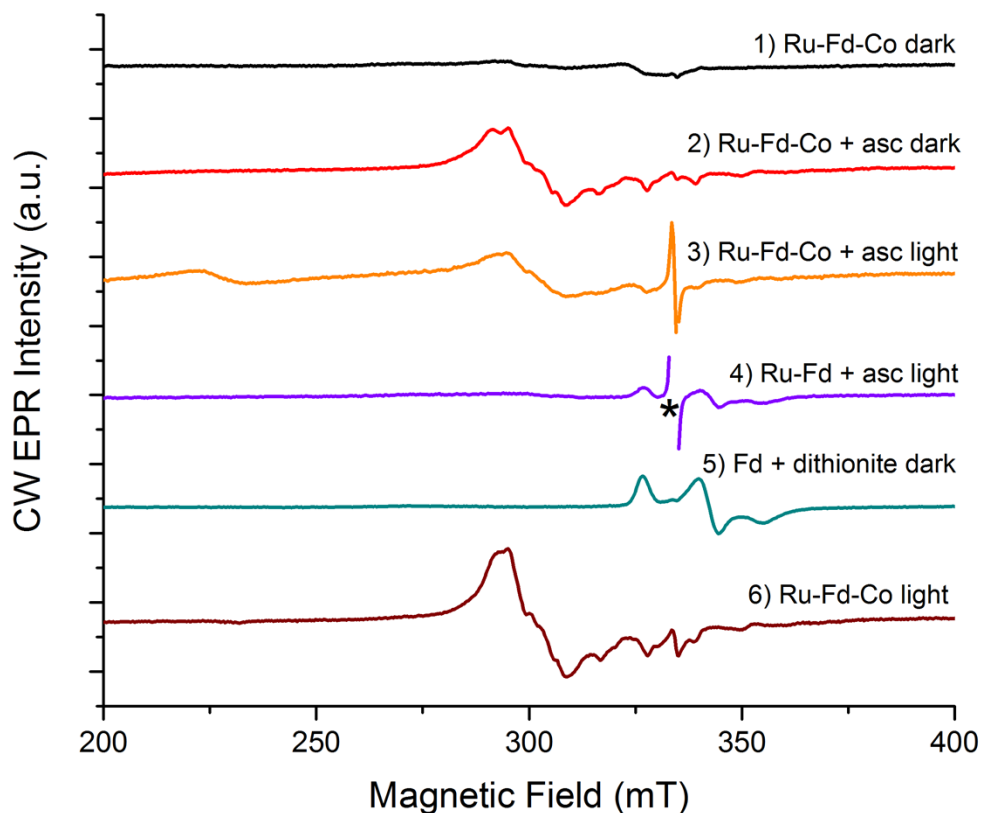


Figure S4: cw X-band EPR spectra of Ru-Fd-Co and Ru-Fd biohybrids. Ru-Fd-Co dark (black 1), Ru-Fd-Co + ascorbate dark (red, 2), Ru-Fd-Co + ascorbate light (orange, 3), Ru-Fd + ascorbate light (violet, 4), Fd + dithionite dark (dark cyan, 5), Ru-Fd-Co light (maroon, 6). “Light” samples were illuminated for 2 s at room temperature followed by immersion in liquid N<sub>2</sub> while illuminated and then placed in a pre-cooled EPR cavity for measurement. All EPR spectra were obtained at 10 K. An asterisk marks a small amount of organic radical generated upon illumination omitted for clarity. The g-values determined for 5 ( $g_x = 2.05$ ,  $g_y = 1.96$ ,  $g_z = 1.89$ ) are typical for ferredoxins.<sup>11</sup> The signal determined for 5 (Fd + dithionite, dark) was scaled by 0.5.

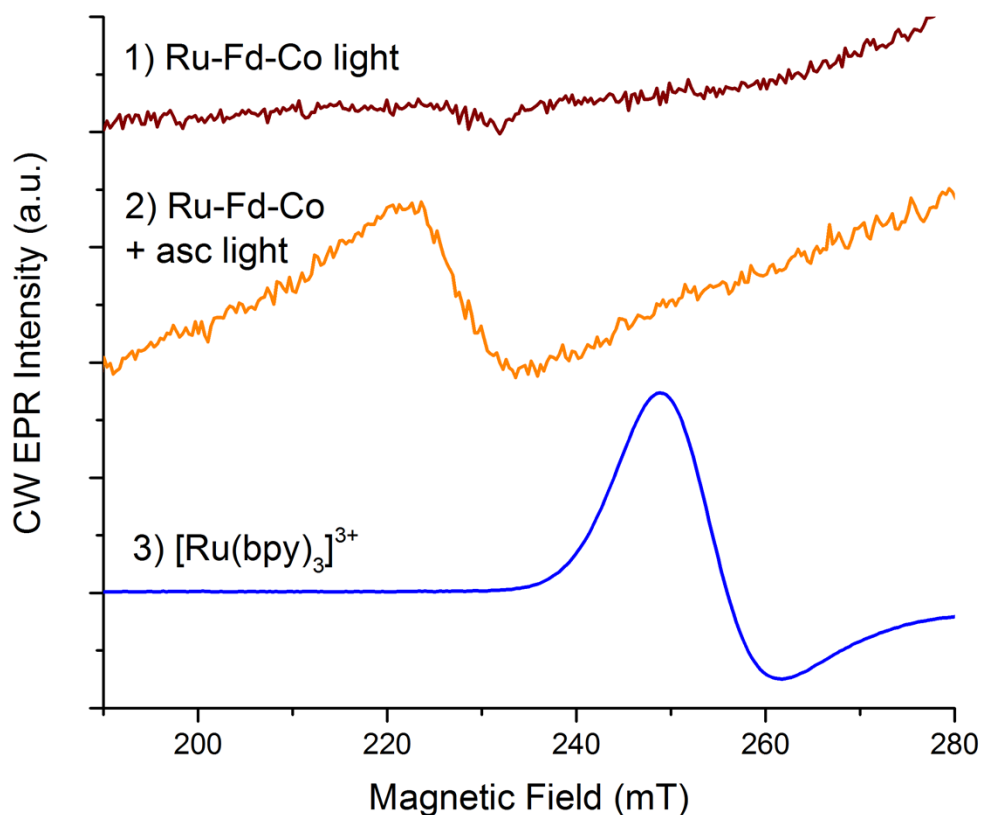


Figure S5: cw X-Band EPR spectra of Ru-Fd-Co after room temperature illumination (orange and maroon), followed by freeze-quenching in liquid N<sub>2</sub>, and placed in the pre-cooled EPR resonator at 10 K. Differences were observed with (orange) or without (maroon) sodium ascorbate (100 mM) in the sample. G-values of Ru(III) features are calculated,  $g = 2.90$  in Ru-Fd-Co frozen under light sample,  $g = 2.95$  in Ru-Fd-Co with ascorbate frozen under light sample. The feature in the Ru-Fd-Co under light sample is transient and decayed within the timescale of recording an EPR spectrum ( $\sim 1$  minute). The model compound [Ru(bpy)<sub>3</sub>]<sup>3+</sup> (blue) was also analyzed as a reference for Ru(III) EPR ( $g = 2.65$ ) consistent with literature values for Ru(III) compounds.<sup>12</sup> The difference in the peak positions is due to the strong dependence of the Ru(III)  $g$ -values on coordination ligands and solvent environment.<sup>12-13</sup> Preparation of the Ru(III)

model compound directly in protein is not feasible. Additionally the Ru(III) model compound has only bipyridyl ligands, while the Ru-Fd-Co complex is ligated to the protein through a cysteine thiolate bond.

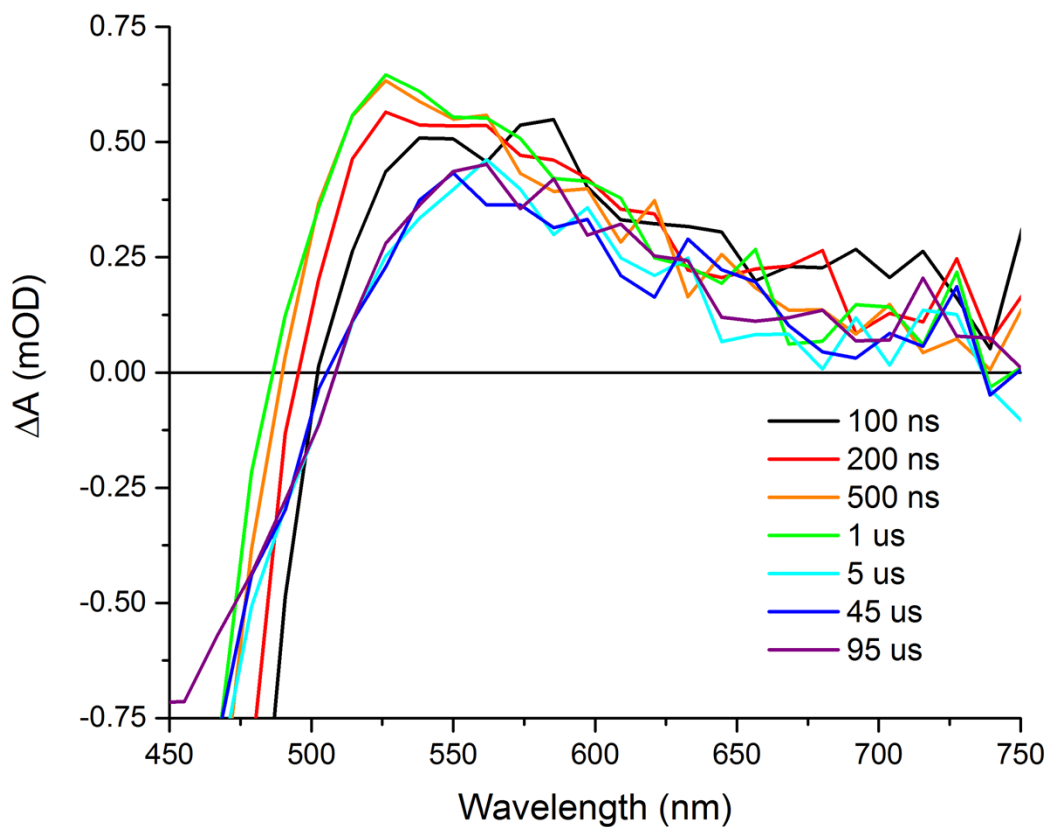


Figure S6. Full spectral transient optical spectra for Ru-Fd-Co with 200 mM sodium ascorbate. Samples were collected with a SpectraPhysics Spitfire Prof Ti:sapphire laser with an EOS automated data collection system (Ultrafast Systems) operating at 1.0 kHz as described in above in the *Experimental Methods*. The pump wavelength was 450 nm and pump power was 600  $\mu$ W. The sample intensity was  $\sim$ 0.3 OD at 450 nm.



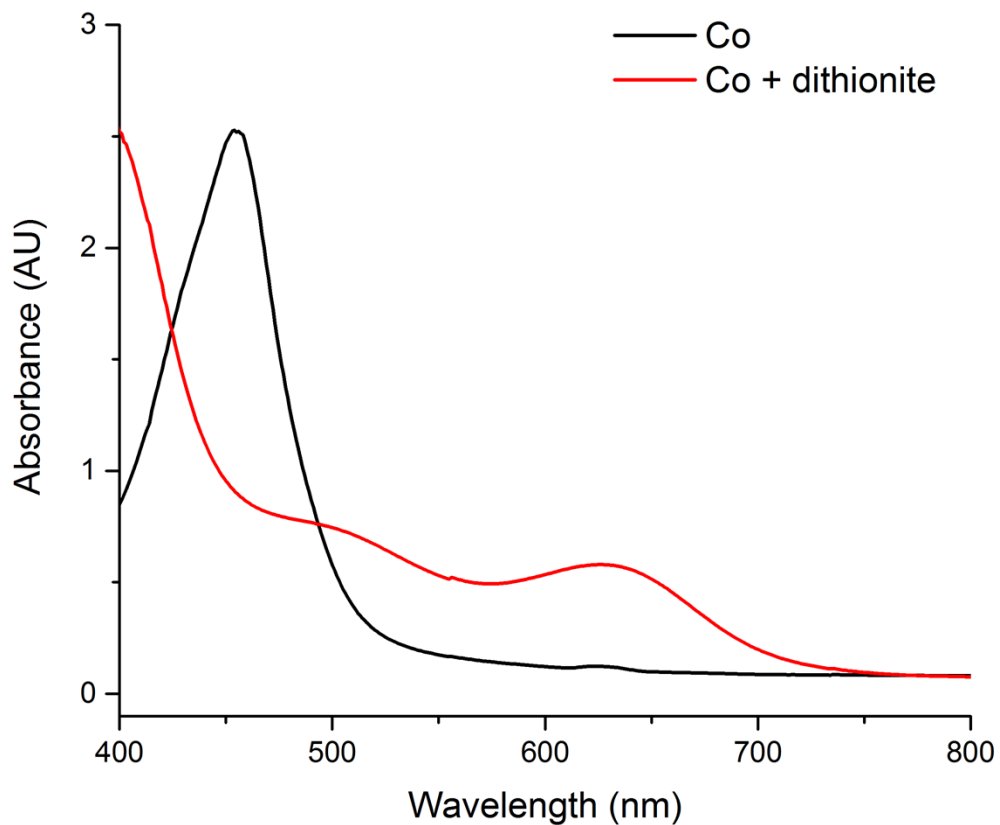


Figure S7: UV-visible absorption spectrum of 500  $\mu\text{M}$  Co catalyst in 20 mM HEPES pH 7.9 (black) and 500  $\mu\text{M}$  Co catalyst in 20 mM HEPES pH 7.9 with 10 mM sodium dithionite (red). The resting Co(II) species (black) has an absorbance maximum at 456 nm, while the reduced Co(I) species (red) has an absorbance maximum of at 638 nm. The Co(I) species is the primary species detected in our transient optical kinetic experiments probed at 660 nm.

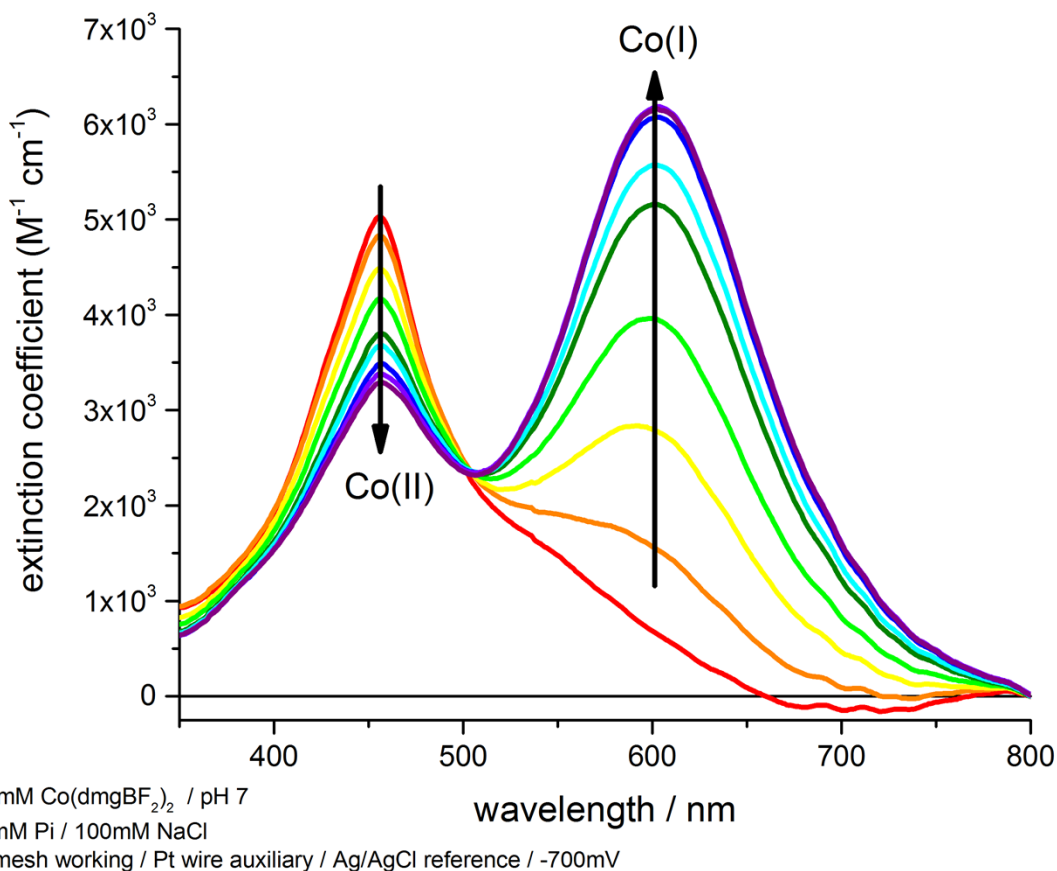


Figure S8: Spectroelectrochemistry of 0.4 mM Co catalyst ( $\text{Co}(\text{dmgBF}_2)_2 \cdot 2\text{H}_2\text{O}$ ) in 10 mM phosphate buffer, pH 7.0 with 100 mM sodium chloride as an electrolyte. The molar extinction coefficient for the Co(I) species is  $\sim 6100 \text{ M}^{-1}\text{cm}^{-1}$  at 600 nm. At 660 nm, the detection wavelength of our experiments, the molar extinction coefficient for the Co(I) species is  $\sim 3500 \text{ M}^{-1}\text{cm}^{-1}$  and is 10 times greater than the extinction coefficient for Ru(III) (Figure S7).

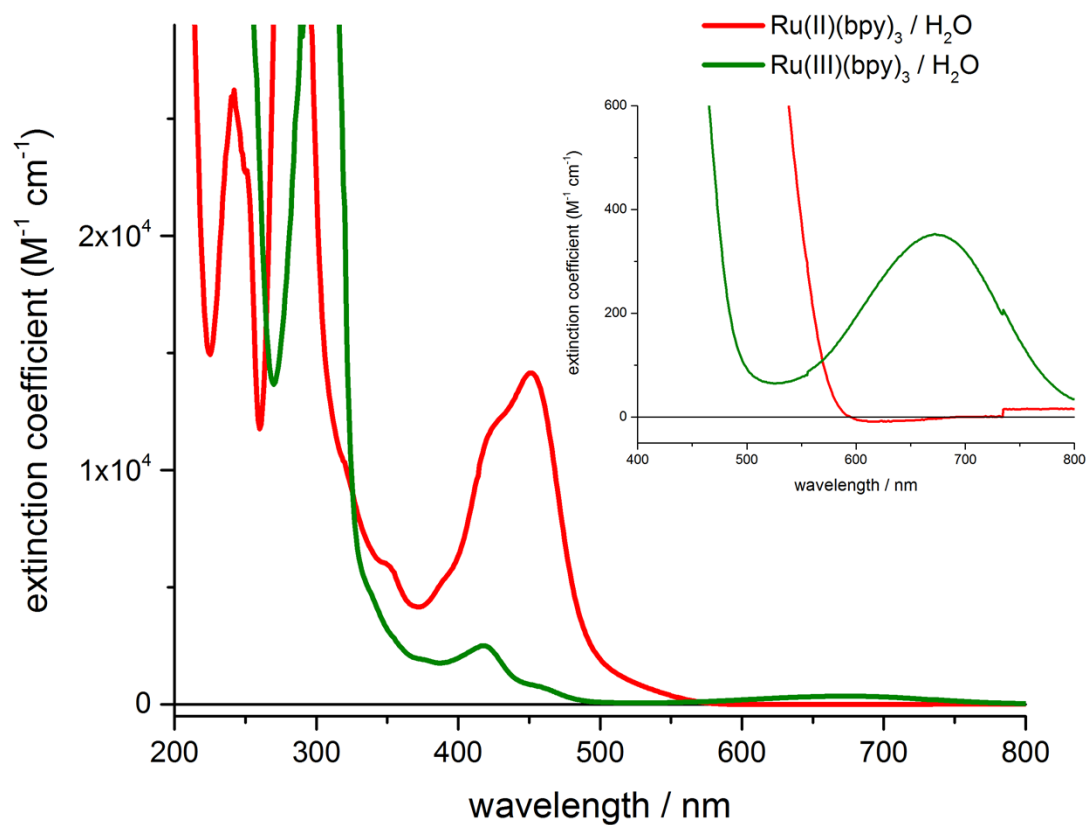


Figure S9: UV-visible absorption spectrum of [Ru(bpy)<sub>3</sub>]<sup>2+</sup> (red) and [Ru(bpy)<sub>3</sub>]<sup>3+</sup> (green) in water. [Ru(bpy)<sub>3</sub>]<sup>3+</sup> is generated as described in the *Experimental Methods* section above and has an absorption peak at 674 nm,  $\epsilon = 350 \text{ M}^{-1}\text{cm}^{-1}$

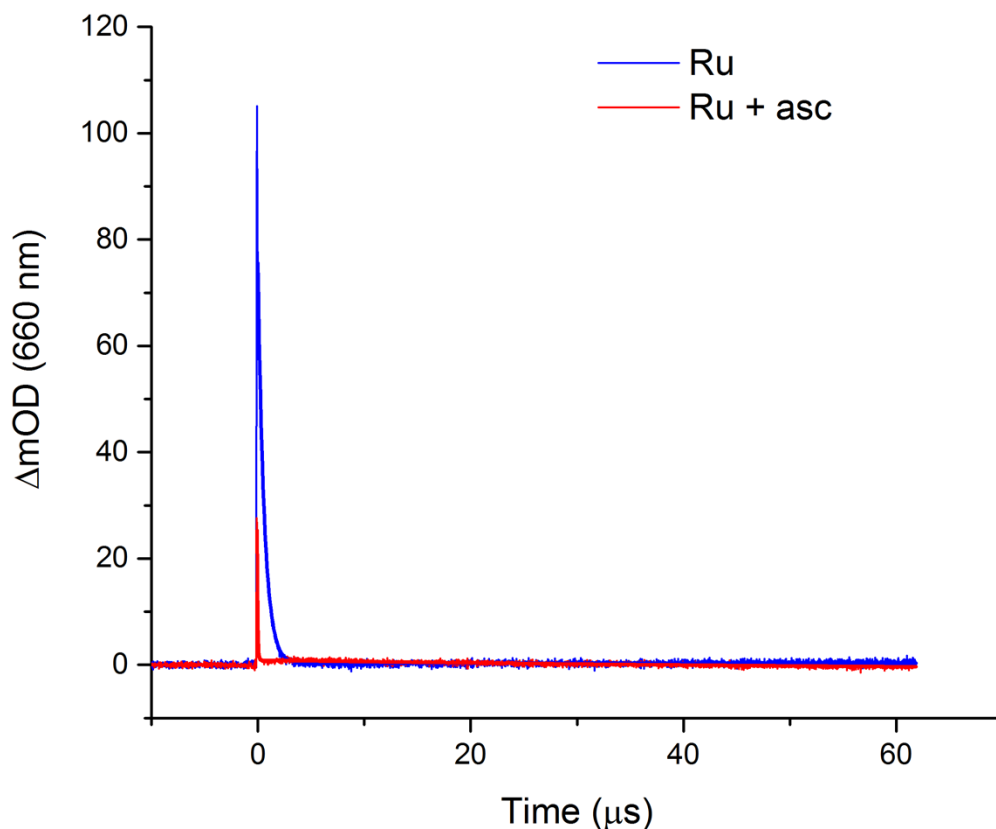


Figure S10: Short time scale transient optical spectroscopy of the model PS,  $[\text{Ru}(\text{bpy})_3] \cdot 2\text{PF}_6$  with and without 200 mM sodium ascorbate. The samples were excited with a 450 nm laser pulse and probed with a 660 nm LED. In the absence of ascorbate, blue, the Ru PS displays a rapid single exponential decay ( $\tau_1 = 0.61 \pm 0.02 \mu\text{s}$ ). Upon the addition of ascorbate, red, we observe an -exponential decay with a very rapid component ( $\tau_1 \sim 0.05 \mu\text{s}$ ) which is fast decay of  $[\text{Ru}(\text{bpy})_3]^{2+*}$  to  $[\text{Ru}(\text{bpy})_3]^+$ .  $[\text{Ru}(\text{bpy})_3]^{2+*}$  has a broad absorption that extends to 660 nm.<sup>14</sup> A faster decay time is observed in the presence of ascorbate (50 ns vs. 600 ns) due to reductive quenching by the ascorbate.

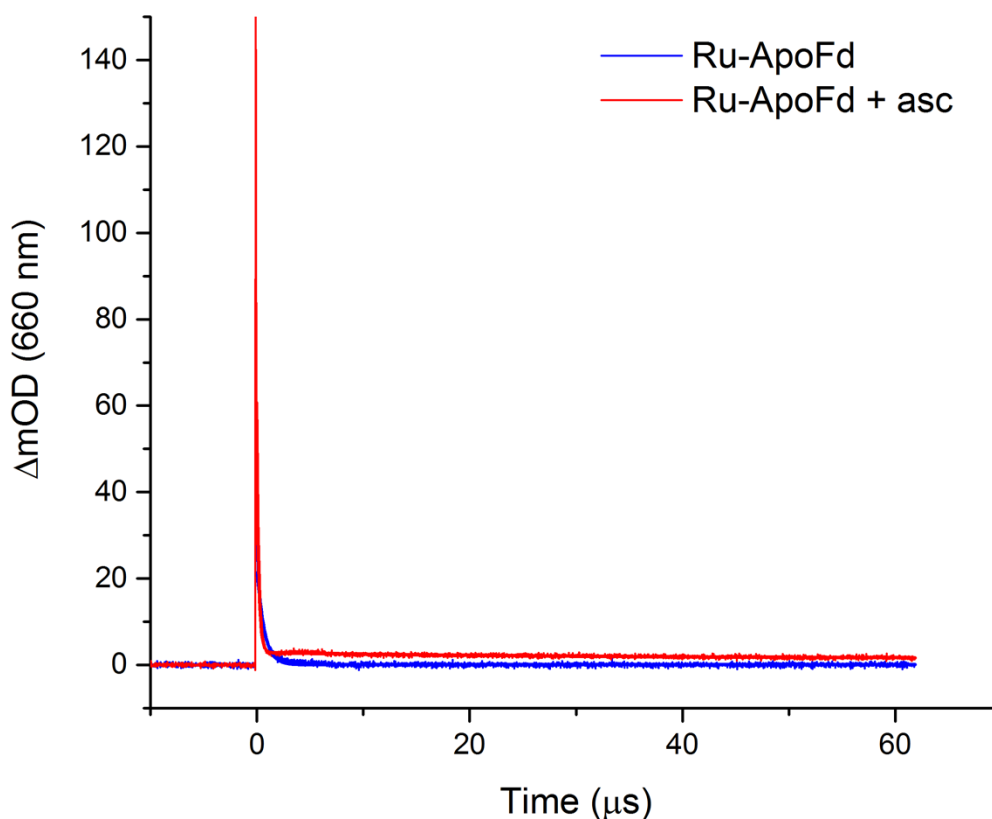


Figure S11: Short time scale transient optical spectroscopy of the Ru-ApoFd biohybrid complex with and with 200 mM sodium ascorbate. The samples were excited with a 450 nm laser pulse and probed with a 660 nm LED. In the absence of the Co catalyst the Ru-ApoFd biohybrid complex behaves similarly to the parent PS,  $[\text{Ru}(\text{bpy})_3]^{2+}$ . In the Ru-ApoFd biohybrid complex in the absence of ascorbate, blue, we observe a single exponential decay ( $\tau_1 = 0.66 \pm 0.07 \mu\text{s}$ ), attributed to  $[\text{Ru}(\text{bpy})_3]^{2+*}$  to  $[\text{Ru}(\text{bpy})_3]^+$  decay. Upon addition of ascorbate, red, we observe a faster exponential decay,  $\tau_1 = 0.20 \pm 0.01 \mu\text{s}$ , attributed to  $[\text{Ru}(\text{bpy})_3]^{2+*}$  to  $[\text{Ru}(\text{bpy})_3]^+$  decay.<sup>15</sup>

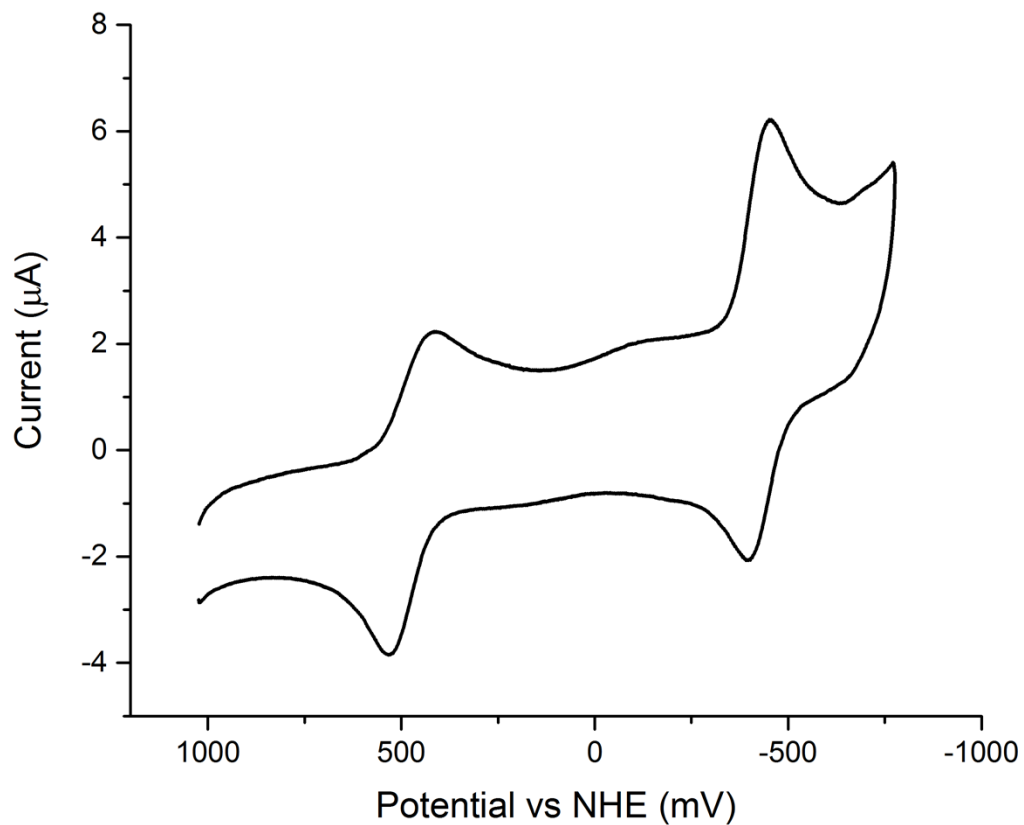


Figure S12: Cyclic voltammogram of Co catalyst ( $\text{Co}(\text{dmgBF}_2)_2 \cdot 2\text{H}_2\text{O}$ ) in 10 mM MES / 100 mM KCl pH 6.3. The midpoint potentials vs. NHE are:  $\text{Co}^{\text{II/I}}$  -0.42 V;  $\text{Co}^{\text{III/II}}$  +0.57 V. Cyclic voltammetry was performed at 100 mV/s using ferrocene carboxylic acid as an internal standard.

## References:

- 1 A. Bakac and J. H. Espenson, *J. Am. Chem. Soc.*, 1984, **106**, 5197.
- 2 (a) L. C. Sun, H. Berglund, R. Davydov, T. Norrby, L. Hammarstrom, P. Korall, A. Borje, C. Philouze, K. Berg, A. Tran, M. Andersson, G. Stenhagen, J. Martensson, M. Almgren, S. Styring and B. Akermark, *J. Am. Chem. Soc.*, 1997, **119**, 6996; (b) S. Gould, G. F. Strouse, T. J. Meyer and B. P. Sullivan, *Inorg. Chem.*, 1991, **30**, 2942.
- 3 E. Liaudet, F. Battaglini and E. J. Calvo, *J. Electroanal. Chem.*, 1990, **293**, 55.
- 4 G. P. McDermott, P. Jones, N. W. Barnett, D. N. Donaldson and P. S. Francis, *Anal. Chem.*, 2011, **83**, 5453.
- 5 G. Moal and B. Lagoutte, *Biochim. Biophys. Acta*, 2012, **1817**, 1635.
- 6 S. C. Silver, J. Niklas, P. Du, O. G. Poluektov, D. M. Tiede and L. M. Utschig, *J. Am. Chem. Soc.*, 2013, **135**, 13246.
- 7 M. M. Bradford, *Anal. Biochem.*, 1976, **72**, 248.
- 8 L. M. Utschig, S. C. Silver, K. L. Mulfort and D. M. Tiede, *J. Am. Chem. Soc.*, 2011, **133**, 16334.
- 9 S. Stoll and A. Schweiger, *J. Magn. Reson.*, 2006, **178**, 42.
- 10 J. Niklas, K. L. Mardis, R. R. Rakhimov, K. L. Mulfort, D. M. Tiede and O. G. Poluektov, *J. Phys. Chem. B*, 2012, **116**, 2943.
- 11 M. Vidakovic, G. Fraczkiewicz, B. C. Dave, R. S. Czernuszewicz and J. P. Germanas, *Biochemistry*, 1995, **34**, 13906.
- 12 K. Matsuura and L. Kevan, *J. Phys. Chem.*, 1996, **100**, 10652.
- 13 (a) A. G. Motten, K. Hanck and M. K. Dearmond, *Chem. Phys. Lett.*, 1981, **79**, 541; (b) S. Sakaki, Y. Yanase, N. Hagiwara, T. Takeshita, H. Naganuma, A. Ohyoshi and K. Ohkubo, *J. Phys. Chem.*, 1982, **86**, 1038.
- 14 Q. Sun, S. Mosquera-Vazquez, L. M. Lawson Daku, L. Guénée, H. A. Goodwin, E. Vauthey and A. Hauser, *J. Am. Chem. Soc.*, 2013, **135**, 13660.
- 15 (a) L. A. Kelly and M. A. J. Rodgers, *J. Phys. Chem.*, 1994, **98**, 6377; (b) B. Shan, T. Baine, X. A. N. Ma, X. Zhao and R. H. Schmechl, *Inorg. Chem.*, 2013, **52**, 4853.